Int. J. Solids Structures Vol. 30, No. 23, pp. 3245–3260, 1993
Printed in Great Britain

0020–7683/93 $6.00+ .00

AN ASYMPTOTIC STRESS ANALYSIS OF LAMINATED PLATES

YIBIN FU
Department of Mathematics, University of Manchester, Oxford Road, Manchester M13 9PL, U.K.

and

ZHENGHUA LI
Department of Mechanical and Process Engineering, The University of Sheffield, Sheffield S1 3JD, U.K.

(*Received* 29 *September* 1992; *in revised form* 30 *April* 1993)

Abstract—For a laminated plate in which each layer is made of a transversely isotropic material, the exact three-dimensional elasticity theory is shown to be greatly simplified with the use of the assumption that the elastic modulus in the preferred direction is large compared with the shear moduli. The resulting asymptotic theory is shown to be best where the classical plate theories fail most: it gives very accurate results for a single-layer thick plate or a thick plate made of only a few layers.

1. INTRODUCTION

It has been well recognized that the classical plate theories are inadequate for the analysis of laminated plates because of their negligence of transverse shear strains. Thus various finite element methods and theories based upon modifying the basic assumptions of the classical plate theories have been proposed in the literature [see Owen and Li (1987), Reddy (1984) and the references therein]. These theories are usually equally suitable for any kind of orthotropic materials. However, many fibre-reinforced composites exhibit the property that the elastic modulus in the fibre direction is large compared with the shear moduli. This property could possibly be exploited to find asymptotic solutions to a variety of stress analysis problems. We start our exploration of this possibility in this paper by first settling the question "how effective could the asymptotic method be in stress analysis of fibre-reinforced composites?" through the consideration of a relatively simple problem. Once this question has been answered, we can then apply the asymptotic method with confidence to more complex problems where exact solutions are not possible.

Asymptotic methods have been widely used in various branches of science in the past 40 years or so and it is well known that they can give very good results even if the underlying large parameters are only moderately large. In the context of stress analysis, asymptotic methods based upon the largeness of the elastic modulus in the fibre direction have been used before in various plane-strain and plane-stress problems and comparisons have been made with known exact solutions where they exist [see e.g. Spencer (1974)]. Pipkin (1979) has written a good review article on this subject. However, as far as we are aware, very few authors have carried out asymptotic stress analysis for three-dimensional problems. Thus examples are still in short supply as to how effective the asymptotic method could be in stress analysis of fibre-reinforced composites and what their limitations are, especially for three-dimensional problems where more length scales are involved. The particular three-dimensional problem considered in this paper has a new feature which is not encountered in plane problems: it involves a small length scale if the thickness of the composing layers are small, which poses a severe test to the asymptotic method. This problem also has an exact solution which enables us to make a critical assessment on the effectiveness of the asymptotic method.

We consider the three-dimensional problem of a laminated plate which is simply supported and which is subject to arbitrary loading on its top and bottom surfaces. We

assume that each layer is made of a transversely isotropic material and the fibres are either aligned with the x-axis or with the y-axis. The exact solution to this problem with each layer made of a general orthotropic material has been given by Pagano (1970), but later we shall show that his formulae are actually not valid for transversely isotropic materials. We will first derive the correct exact solutions and then compare the asymptotic solutions with them by considering two specific examples.

This paper is divided into seven sections as follows. In the next section, we first consider a single layer and derive the asymptotic solutions for the stress and displacement fields and then we show how to construct the global solutions. In Section 3 we give the modified form of Pagano's (1970) exact solution appropriate to transversely isotropic materials, which is followed in Section 4 by an improved formulation based on the propagator matrix method (Gilbert and Backus, 1966). In Section 5, we consider two specific examples and compare our asymptotic results with the exact solutions. The dependence of our asymptotic results on the values of elastic moduli and the layer thickness is further discussed in Section 6. In the final section, we draw some conclusions.

2. THE THREE-DIMENSIONAL ASYMPTOTIC SOLUTION FOR A SINGLE LAYER

Consider a laminated rectangular plate ($0 \leqslant x \leqslant a, 0 \leqslant y \leqslant b, 0 \leqslant z \leqslant h$) composed of N transversely isotropic layers such that the preferred direction (i.e. the fibre direction) of each layer is either along the x-axis or along the y-axis. We assume that the four sides are simply supported and are traction-free. The boundary conditions on the top and bottom surfaces are assumed to be arbitrary at the moment and will be specified when we consider specific problems. In order to determine the displacement and stress fields in this plate, we first focus our attention on a single layer which has its preferred direction along the x-axis. For such a layer, the constitutive equations are given by [see Spencer (1984)]

$$\begin{Bmatrix} \sigma_x \\ \sigma_y \\ \sigma_z \end{Bmatrix} = \begin{bmatrix} \beta & \lambda+\alpha & \lambda+\alpha \\ \lambda+\alpha & \lambda+2\mu_t & \lambda \\ \lambda+\alpha & \lambda & \lambda+2\mu_t \end{bmatrix} \begin{Bmatrix} e_{xx} \\ e_{yy} \\ e_{zz} \end{Bmatrix}, \tag{1}$$

$$\tau_{yz} = 2\mu_t e_{yz}, \quad \tau_{xz} = 2\mu_l e_{xy}, \quad \tau_{xy} = 2\mu_l e_{xy}. \tag{2}$$

Here μ_l and μ_t are shear moduli for shear on planes parallel to the fibres, with direction of shear in the fibre direction (μ_l) and normal to the fibre direction (μ_t) respectively. The extension moduli E_l for uniaxial tension in the fibre direction and E_t for uniaxial tension in directions normal to the fibres and the Poisson's ratio ν_{lt} are related to λ, α and β by (Spencer, 1974):

$$E_l = \beta - \frac{(\lambda+\alpha)^2}{\lambda+\mu_t}, \quad E_t = \frac{4\mu_t[\beta(\lambda+\mu_t)-(\lambda+\alpha)^2]}{(\lambda+2\mu_t)\beta-(\lambda+\alpha)^2}, \quad \nu_{lt} = \frac{\lambda+\alpha}{2(\lambda+\mu_t)}. \tag{3}$$

Here ν_{lt} measures strain in the t-direction under uniaxial normal stress in the fibre direction; whilst the other Poisson's ratio ν_{tt} can be calculated from $\nu_{tt} = E_t/(2\mu_t) - 1$ due to transverse isotropy.

In this paper, we formulate our problem in terms of the displacement (u, v, w). On substituting the strain-displacement relations into (1) and (2) and then the resulting expressions into the equations of equilibrium, we obtain

$$\beta u_{,xx} + \mu_l(u_{,yy}+u_{,zz}) + (\lambda+\alpha+\mu_l)v_{,xy} + (\lambda+\alpha+\mu_l)w_{,xz} = 0, \tag{4}$$

$$\mu_l v_{,xx} + (\lambda+2\mu_t)v_{,yy} + \mu_t v_{,zz} + (\lambda+\alpha+\mu_l)u_{,xy} + (\lambda+\mu_t)w_{,yz} = 0, \tag{5}$$

$$\mu_l w_{,xx} + \mu_t w_{,yy} + (\lambda+2\mu_t) w_{,zz} + (\lambda+\alpha+\mu_l) u_{,xz} + (\lambda+\mu_t) v_{,yz} = 0. \tag{6}$$

Here a comma denotes partial differentiation.

Following Pagano (1970), we look for the following "normal mode solutions" to the above equations:

$$\begin{aligned} u &= U(z) \cos px \sin qy, \\ v &= V(z) \sin px \cos qy, \\ w &= W(z) \sin px \sin qy, \end{aligned} \tag{7}$$

where

$$p = \frac{n\pi}{a}, \quad q = \frac{m\pi}{b}, \quad (n, m = 1, 2, \ldots). \tag{8}$$

Once the above forms of the solutions have been found, a double Fourier expansion will then be able to satisfy any boundary or interface conditions. We note that the expressions (7) have already satisfied the simple support edge conditions.

In order to find the differential equations satisfied by U, V and W, we substitute (7) into (4)–(6) and obtain

$$-p^2\beta U + \mu_l(U'' - q^2 U) - (\lambda+\alpha+\mu_l) pqV + (\lambda+\alpha+\mu_l) pW' = 0, \tag{9}$$

$$-\mu_l p^2 V - (\lambda+2\mu_t) q^2 V + \mu_t V'' - (\lambda+\alpha+\mu_l) pqU + (\lambda+\mu_t) qW' = 0, \tag{10}$$

$$-\mu_l p^2 W - \mu_t q^2 W + (\lambda+2\mu_t) W'' - (\lambda+\alpha+\mu_l) pU' - (\lambda+\mu_t) qV' = 0. \tag{11}$$

Here a prime denotes differentiation with respect to z. This set of equations has been solved exactly by Pagano (1970). Here we shall solve them using the asymptotic method, aiming to simplify the analysis and also to assess the accuracy of the asymptotic method.

The first task in an asymptotic analysis is to non-dimensionalize the governing equations using appropriate scales and to identify the sizes of all dimensionless parameters. Here we use μ_l to scale the elastic constants and use the layer thickness, $\tilde{h}$ say, to scale the variable z. Then the non-dimensional version of the governing equations (9)–(11), which will not be written out here, would involve the following three parameters whose sizes need to be fixed:

$$\varepsilon = \frac{\mu_l}{\beta}, \quad s = \frac{\pi}{p\tilde{h}} = \frac{a}{n\tilde{h}}, \quad r = \frac{q}{p} = \frac{ma}{nb}. \tag{12}$$

For many advanced composites like graphite-epoxy, ε is of the order 0.02. In the following mathematical development, ε is assumed to be infinitesimally small (in view of the relation (3a), this is equivalent to assuming that the Young's modulus E_l is large compared with the shear modulus μ_l), whilst the other two parameters s and r are assumed to be of order one relative to ε. The effect of the latter assumption on the accuracy of the asymptotic results will be discussed in the final section.

Based on these assumptions, we look for the following form of asymptotic solutions for (9)–(11):

$$U = U_0 + \varepsilon U_1 + \cdots, \quad V = V_0 + \varepsilon V_1 + \cdots, \quad W = W_0 + \varepsilon W_1 + \cdots. \tag{13}$$

Although in theory the above asymptotic expressions can approximate the exact solution to any desired order of degree if enough higher order terms are retained, we shall mainly be concerned with the leading order solutions in the present paper.

On substituting (13) into (9)–(11), replacing β in (9) by μ_l/ε and then equating the coefficients of like powers of ε, we obtain a hierarchy of differential equations for U_0, U_1, etc. To leading order, (9)–(11) in turn give

$$U_0 = 0, \tag{14}$$

$$\mu_l p^2 V_0 + (\lambda+2\mu_t)q^2 V_0 - \mu_t V_0'' - (\lambda+\mu_t)qW_0' = 0, \tag{15}$$

$$-(\mu_l p^2 + \mu_t q^2)W_0 + (\lambda+2\mu_t)W_0'' - (\lambda+\mu_t)qV_0' = 0. \tag{16}$$

By differentiating (16) and using (15) to eliminate W_0, we obtain

$$\mu_t(\lambda+2\mu_t)V_0^{(4)} - \{(\lambda+3\mu_t)\mu_l p^2 + (2\lambda\mu_t + 4\mu_t^2)q^2\}V_0'' + (\mu_l p^2 + \mu_t q^2)[\mu_l p^2 + (\lambda+2\mu_t)q^2]V_0 = 0. \tag{17}$$

We note that the order of this equation is four whilst the order of the equation satisfied by the exact solution for V should be six [see Pagano (1970)]. Thus in the limit $\varepsilon \to 0$, the highest derivative term has been dropped. This is certainly typical of asymptotic analysis. Because of the reduction of the order of the governing equation, we cannot expect the corresponding leading order solution to satisfy all of the boundary and interface conditions. The latter conditions can be satisfied by the boundary layer solutions to be introduced later.

It is easy to show that the general solution of (17) is given by

$$V_0(z) = C_1 e^{\sigma_1 z} + C_2 e^{-\sigma_1 z} + C_3 e^{\sigma_2 z} + C_4 e^{-\sigma_2 z}, \tag{18}$$

where C_1, C_2, C_3 and C_4 are disposable constants and $\sigma_{1,2}$ have the explicit expressions

$$\sigma_1 = \sqrt{\frac{\mu_l}{\mu_t}p^2 + q^2}, \quad \sigma_2 = \sqrt{\frac{\mu_l}{\lambda+2\mu_t}p^2 + q^2}. \tag{19}$$

These explicit expressions, obtained under the small ε limit, are significant simplifications over Pagano's exact expressions (later we will see that (19a) is in fact exact).

The expression for W_0 is obtained by integrating (15) and is given by

$$(\lambda+\mu_t)qW_0(z) = \left(\frac{\omega(p,q)}{\sigma_1^2} - \mu_t\right)\sigma_1(C_1 e^{\sigma_1 z} - C_2 e^{-\sigma_1 z}) + \left(\frac{\omega(p,q)}{\sigma_2^2} - \mu_t\right)\sigma_2(C_3 e^{\sigma_2 z} - C_4 e^{-\sigma_2 z}), \tag{20}$$

where the arbitrary integration constant has been set to zero in order to satisfy (16) [note that (17) has been obtained by differentiating (16)] and the function $\omega(p,q)$ is defined by

$$\omega(p,q) = \mu_l p^2 + (\lambda+2\mu_t)q^2. \tag{21}$$

Since $U_0 = 0$, the function U is in fact of order ε and U_1 then becomes important [see (13a)]. To determine U_1, we equate the coefficients of ε^0 in (9) and obtain

$$U_1 = \frac{\lambda+\alpha+\mu_l}{\mu_l p}(W_0' - qV_0).$$

If we introduce five more functions through

$$\omega_1(p,q) = \sigma_1 = \sqrt{\frac{\mu_l}{\mu_t}p^2+q^2}, \quad \omega_2(p,q) = -\sigma_1,$$

$$\omega_3(p,q) = \sigma_2 = \sqrt{\frac{\mu_l}{\lambda+2\mu_t}p^2+q^2}, \quad \omega_4(p,q) = -\sigma_2,$$

$$F(\omega,\sigma,z) = \frac{1}{\lambda+\mu_t}\left[\frac{\omega(p,q)}{\sigma^2}-\mu_t\right]\sigma\, e^{\sigma z}, \tag{22}$$

then the leading order solution obtained above can be neatly written as

$$U(z) = \varepsilon\cdot\frac{\lambda+\alpha+\mu_l}{\mu_l pq}\sum_{i=1}^{4}(\omega_i F(\omega,\omega_i,z)-q^2\, e^{\omega_i z})C_i,$$

$$V(z) = \sum_{i=1}^{4} C_i\, e^{\omega_i z},$$

$$W(z) = \frac{1}{q}\sum_{i=1}^{4} C_i F(\omega,\omega_i,z). \tag{23}$$

These expressions have the nice property that each differentiation only produces a factor ω_i under the summation sign.

2.1. *Boundary layer solutions*

The leading order solution (23) contains only four disposable constants and so it cannot in general satisfy the six boundary or interface conditions. This is due to the negligence of the term $\mu_l U''$ in (9) in our leading order approximation. This term can be neglected if $\partial/\partial z$ is not large. Thus the solution (23) is only valid in the inner region (away from the two surfaces of the layer under consideration) where the z-variation is of order ε^0. However, near the two surfaces of the layer, $U(z)$ has to vary rapidly so as to adjust to the conditions at the surfaces. From (9) we see that the thicknesses of these "boundary layers" are determined from the condition that

$$\frac{\partial^2}{\partial z^2} = O\left(\frac{1}{\varepsilon}\right).$$

Thus the boundary layer thickness is of order $\varepsilon^{1/2}$ and so we introduce two boundary layer variables

$$\xi_1 = \frac{z-h_1}{\varepsilon^{1/2}} \quad \text{and} \quad \xi_2 = \frac{z-h_2}{\varepsilon^{1/2}}, \tag{24}$$

which are appropriate to the lower surface ($z = h_1$) and upper surface ($z = h_2$), respectively. For the boundary layer near the lower surface, we look for solutions of the form

$$U = \varepsilon^{1/2}\hat{U}_0(\xi_1)+\varepsilon\hat{U}_1(\xi_1)+\cdots,$$
$$V = \hat{V}_0(\xi_1)+\varepsilon^{1/2}\hat{V}_1(\xi_1)+\cdots,$$
$$W = \hat{W}_0(\xi_1)+\varepsilon^{1/2}(\xi_1)+\cdots. \tag{25}$$

Here we have anticipated U to be of order $\varepsilon^{1/2}$, since we expect $\sigma_{zz}(=O(U'))$ to be $O(1)$.

On transforming the independent variable z to ξ_1 in (9)–(11) with the use of (24a), substituting (25) into the resulting equations and then equating the coefficients of like powers of ε, we obtain

$$\hat{V}_0''(\xi_1) = \hat{V}_1''(\xi_1) = \hat{W}_0''(\xi_1) = \hat{W}_1''(\xi_1) = 0 \tag{26}$$

and

$$\hat{U}_0''(\xi_1) - p^2 \hat{U}_0(\xi_1) = 0, \tag{27}$$

$$\hat{U}_1''(\xi_1) - p^2 \hat{U}_1(\xi_1) = \frac{p(\lambda+\alpha+\mu_l)}{\mu_l}[q\hat{V}_0(\xi_1) - \hat{W}_1'(\xi_1)]. \tag{28}$$

By solving (26) subject to the condition that the boundary layer solution (25) should match with the inner solution (23), we find that

$$\hat{V}_0 = V_0(h_1), \quad \hat{V}_1(\xi_1) = V_0'(h_1)\xi_1,$$
$$\hat{W}_0(\xi_1) = W_0(h_1), \quad \hat{W}_1(\xi_1) = W_0'(h_1)\xi_1.$$

Inserting these expressions back into (25b,c) then shows that the boundary layer solution for V and W is simply the inner solution expanded in the neighbourhood of the lower surface. Thus the boundary layer has a passive role with regard to the determination of V and W. As for U, solving (27) gives $\hat{U}_0(\xi_1) = C_5 e^{-p\xi_1} + C_7 e^{p\xi_1}$. As we move away from the lower surface into the inner region (i.e. as $\xi_1 \to \infty$), $\hat{U}_0(\xi_1)$ should tend to zero in order to match with the inner solution (23a). Thus $C_7 = 0$ and

$$\hat{U}_0(\xi_1) = C_5 e^{-p\xi_1}. \tag{29}$$

With similar considerations, we solve (28) to obtain

$$\hat{U}_1(\xi_1) = \frac{\lambda+\alpha+\mu_l}{\mu_l p}[W_0'(h_1) - qV_0(h_1)], \tag{30}$$

where the term proportional to $e^{-p\xi_1}$ has been set to zero since otherwise it can be absorbed into $\hat{U}_0$ by redefining the constant C_5.

In a similar fashion, we can show that in the neighborhood of the upper surface, the boundary layer solution for V and W is simply the inner solution expanded about $z = h_2$ and U expands like $U = \varepsilon^{1/2}\hat{\hat{U}}_0(\xi_2) + \varepsilon\hat{\hat{U}}_1(\xi_2) + \cdots$ with $\hat{\hat{U}}_0$ and $\hat{\hat{U}}_1$ given by

$$\hat{\hat{U}}_0(\xi_2) = C_6 e^{p\xi_2}, \quad \hat{\hat{U}}_1(\xi_2) = \frac{(\lambda+\alpha+\mu_l)}{\mu_l p}[W_0'(h_2) - qV_0(h_2)]. \tag{31}$$

Thus by considering the boundary layer solutions, we have brought the total number of disposable constants up to six, which is the right number for satisfying all the possible boundary and interface conditions.

Once we have obtained the inner and boundary layer solutions, the composite solution (valid throughout the ply) can be constructed in the usual manner (Nayfeh, 1973) and is given by, with higher order terms neglected,

$$U = \varepsilon^{1/2}(C_5 e^{-p\xi_1} + C_6 e^{p\xi_2}) + \varepsilon \cdot \frac{\lambda+\alpha+\mu_l}{\mu_l pq} \sum_{i=1}^{4} (\omega_i F(\omega, \omega_i, z) - q^2 e^{\omega_i z}) C_i,$$

$$V = \sum_{i=1}^{4} C_i e^{\omega_i z},$$

$$W = \frac{1}{q} \sum_{i=1}^{4} C_i F(\omega, \omega_i, z). \tag{32}$$

We note that in the inner region, $e^{-p\xi_1}$ and $e^{p\xi_2}$ are both exponentially small and (32)

reduces to the inner solution (23); whilst in the upper (lower) layer, $e^{-p\xi_1}(e^{p\xi_2})$ is exponentially small and (32) reduces to the boundary layer solution in the upper (lower) layer. Thus (32) is indeed valid throughout the ply.

2.2. *Stress field*

With the use of (32) and (1), the stress components in the single layer under consideration are found to leading order to be given by

$$\sigma_x = \{-\mu_l p(C_5 e^{-p\xi_1} + C_6 e^{p\xi_2})\varepsilon^{-1/2} - \frac{\mu_l}{q}\sum_{i=1}^{4}[\omega_i F(\omega,\omega_i,z) - q^2 e^{\omega_i z}]C_i\}\sin px \sin qy, \tag{33}$$

$$\sigma_y = \sum_{i=1}^{4}\left\{\frac{\lambda\omega_i}{q}F(\omega,\omega_i,z) - (\lambda+2\mu_t)q e^{\omega_i z}\right\}C_i \sin px \sin qy, \tag{34}$$

$$\sigma_z = \sum_{i=1}^{4}\left\{\frac{\lambda+2\mu_t}{q}\omega_i F(\omega,\omega_i,z) - \lambda q e^{\omega_i z}\right\}C_i \sin px \sin qy, \tag{35}$$

$$\tau_{yz} = \mu_t \sum_{i=1}^{4}\{F(\omega,\omega_i,z) + \omega_i e^{\omega_i z}\}C_i \sin px \cos qy, \tag{36}$$

$$\tau_{xz} = \mu_l p\left\{-C_5 e^{-p\xi_1} + C_6 e^{p\xi_2} + \frac{1}{q}\sum_{i=1}^{4} C_i F(\omega,\omega_i,z)\right\}\cos px \sin qy, \tag{37}$$

$$\tau_{xy} = \mu_l p\left(\sum_{i=1}^{4} e^{\omega_i z} C_i\right)\cos px \cos qy. \tag{38}$$

On substituting (32) into (7), we obtain the displacement field

$$u = \varepsilon^{1/2}\left\{(C_5 e^{-p\xi_1} + C_5 e^{p\xi_2}) + \varepsilon^{1/2}\cdot\frac{\lambda+\alpha+\mu_l}{\mu_l pq}\sum_{i=1}^{4}(\omega_i F(\omega,\omega_i,z) - q^2 e^{\omega_i z})C_i\right\}\cos px \sin qy, \tag{39}$$

$$v = \left(\sum_{i=1}^{4} C_i e^{\omega_i z}\right)\sin px \cos qy,$$

$$w = \frac{1}{q}\left(\sum_{i=1}^{4} C_i F(\omega,\omega_i,z)\right)\sin px \sin qy. \tag{40}$$

The above solutions are for a single layer which has its preferred direction along the x-axis. For a layer which has its preferred direction aligned with the y-axis, the displacement and stress fields can be obtained from (33)–(40) by replacing (p,q) by (q,p), (x,y) by (y,x), (u,v) by (v,u) and leaving others unchanged.

For a single-layer plate, the six constants C_i $(i = 1,2,\ldots,6)$ are determined by the six boundary conditions on the top and bottom surfaces. For a plate made of N (say) layers, the six boundary conditions are augmented by $6(N-1)$ interface continuity conditions. This system is sufficient to solve for the $6N$ unknown constants C_{ik} $(i = 1,\ldots,6;$ $k = 1,\ldots,N)$ (where an additional subscript k is introduced to identify the kth layer). Once these constants are determined, the displacement and stress fields can be calculated by using the appropriate relations given in this section. The determination of the $6N$ constants C_{ik}

involves the assembly and inversion of a $6N \times 6N$ matrix. In Section 4, we shall give an improved formulation which only involves the inversion of a series of 6×6 matrices.

3. THE EXACT SOLUTION

As we have remarked in the Introduction, the problem solved in the preceding section by an asymptotic method has been solved before by Pagano (1970) for general orthotropic materials, but his solution is not valid for transversely isotropic materials. In this section, the appropriate formulae will be derived.

For easy reference, we shall prefix the equation numbers in Pagano's (1970) paper by a letter "P" wherever they are referred to hereafter. For transversely isotropic materials, it can be shown that the constant J_3 defined by (P22c) vanishes and hence L_3 and R_3 appearing in (P22a,b) are not properly defined. It can also be shown that the constant m_3 defined by (P21) reduces to

$$m_3 = \sqrt{\frac{c_{55}}{c_{44}}p^2 + q^2}, \tag{41}$$

which is, surprisingly, identically equal to σ_1 defined by (19) (which is obtained in the small ε limit). The eigenrelations [defined by (P9)] corresponding to m_3 can be shown to be given by

$$U^0 = 0, \quad qV^0 - m_3 W^0 = 0, \tag{42}$$

where (U^0, V^0, W^0) are defined by (P8) and appear in (P9). Since Pagano's formulae require U^0 to be non-zero, modifications have to be made. It can be shown that (P18) should now be replaced by

$$U(z) = \sum_{j=1}^{3} S_j U_j(z), \quad V(z) = \sum_{j=1}^{3} L_j U_j(z), \quad W(z) = \sum_{j=1}^{3} R_j W_j(z), \tag{43}$$

where the constants L_j, R_j $(j = 1, 2)$ are defined by (P22), the functions U_j and W_j are given by (P19) and

$$S_1 = S_2 = 1, \quad S_3 = 0, \quad L_3 = 1, \quad R_3 = \frac{q}{m_3}. \tag{44}$$

Consequently, eqns (P19) and (P23a,b) remain unchanged, but (P23c,d) and (P24) should be replaced by

$$\begin{aligned}
\tau_{xz} &= c_{55} \cos px \sin qy \sum_{j=1}^{3} (S_j m_j + pR_j) W_j(z), \\
\tau_{xy} &= c_{66} \cos px \cos qy \sum_{j=1}^{3} (S_j q + pL_j) U_j(z), \\
M_{ij} &= -pC_{1i} S_j - qC_{2i} L_j + \alpha_j m_j R_j C_{3i}, \quad (i, j = 1, 2, 3).
\end{aligned} \tag{45}$$

These modified expressions together with those of Pagano's (1970) original formulae which remain unchanged constitute the exact solution to a single layer which is made of a transversely isotropic material with its preferred direction aligned with the x-axis. To apply the above formulae to general orthotropic materials, we simply let $S_1 = S_2 = S_3 = 1$ (and we then recover Pagano's original formulae).

4. AN IMPROVED FORMULATION

Once the exact solution for each layer has been found, the usual approach for finding the global solution would involve the assembly and inversion of a $6N \times 6N$ matrix derived from the boundary and interface conditions, as we have indicated at the end of Section 2. Although the inversion of a large matrix can be done easily nowadays using high-speed computers, the assembly of this large matrix remains a laborious task and is prone to errors. In this section, we give an improved formulation which is based upon the propagator matrix method (Gilbert and Backus, 1966). The latter method has been commonly used in solving wave propagation problems, but does not seem to have been employed in the solution of static problems. We shall only write down the formulation for the exact theory since the improved formulation is at its best when the number of layers becomes large and for this type of problem the asymptotic theory is not very suitable, as we will show in the following sections.

We start our formulation by first noting that if we define two vectors $\boldsymbol{\alpha}$ and $\boldsymbol{\beta}(z)$ through

$$\boldsymbol{\alpha} = \begin{Bmatrix} F_1 \\ G_1 \\ \vdots \\ F_3 \\ G_3 \end{Bmatrix}, \quad \boldsymbol{\beta}(z) = \begin{Bmatrix} U(z) \\ V(z) \\ W(z) \\ \hat{\tau}_{xz}(z) \\ \hat{\tau}_{yz}(z) \\ \hat{\sigma}_z(z) \end{Bmatrix}, \tag{46}$$

where

$$\hat{\tau}_{xz} = \frac{\tau_{xz}}{\cos px \sin qy}, \quad \hat{\tau}_{yz} = \frac{\tau_{yz}}{\sin px \cos qy}, \quad \hat{\sigma}_z = \frac{\sigma_z}{\sin px \sin qy}, \tag{47}$$

and F_j, G_j $(j = 1, 2, 3)$ are the six constants appearing in (P18), then (43), (45a) and (P23c,d) can be written as

$$\boldsymbol{\beta}(z) = \mathbf{A}(z)\boldsymbol{\alpha}, \tag{48}$$

where the 6×6 components of $\mathbf{A}$ can be read off from the appropriate equations. Similarly, if we define another vector $\boldsymbol{\gamma}(z)$ by

$$\boldsymbol{\gamma}(z) = \begin{Bmatrix} \hat{\tau}_{xy} \\ \hat{\sigma}_y \\ \hat{\sigma}_z \end{Bmatrix}, \tag{49}$$

where

$$\hat{\tau}_{xy} = \frac{\tau_{xy}}{\cos px \cos qy}, \quad \hat{\sigma}_x = \frac{\sigma_x}{\sin px \sin qy}, \quad \hat{\sigma}_y = \frac{\sigma_y}{\sin px \sin qy}, \tag{50}$$

then (P23a,b,f) can be written as

$$\boldsymbol{\gamma}(z) = \mathbf{B}(z)\boldsymbol{\alpha}, \tag{51}$$

where $\mathbf{B}$ is a 3×6 matrix and its 18 components can be read off from (P23a,b,f).

Suppose now z_1 and z_2 are two arbitrary points in a layer. Equation (48) then gives two relations at these two points. On eliminating $\boldsymbol{\alpha}$ from these relations, we obtain

$$\boldsymbol{\beta}(z_2) = \mathbf{P}(z_2, z_1)\boldsymbol{\beta}(z_1), \tag{52}$$

where $\mathbf{P}(z_2, z_1) = \mathbf{A}(z_2)\mathbf{A}^{-1}(z_1)$. Eliminating α from (48) and (51) yields

$$\gamma(z) = \mathbf{B}(z)\mathbf{A}^{-1}(z)\boldsymbol{\beta}(z). \tag{53}$$

The matrix $\mathbf{P}$, called the propagator matrix, has the following properties: for arbitrary values of z in the layer, say z_1, z_2 and z_3,

$$\mathbf{P}(z_2, z_1) = \mathbf{P}^{-1}(z_1, z_2) \tag{54}$$

and

$$\mathbf{P}(z_3, z_1) = \mathbf{P}(z_3, z_2)\mathbf{P}(z_2, z_1). \tag{55}$$

Both these relations can be deduced from (52). From (54), $\mathbf{P}(z_1, z_1)$ is the identity matrix. From (55) it can be shown that the linear relation between the vector $\boldsymbol{\beta}$ at any two points in a given layer is independent of the origin of z and is, in fact, dependent only on the distance between the two points. Thus

$$\mathbf{P}(z_2, z_1) = \mathbf{P}(z_2 - z_1, 0). \tag{56}$$

We now assume that the interfaces of the N layers are at $z = z_1, z_2, \ldots, z_{N-1}$ (the bottom and top surfaces are at $z = 0, h$). With the repeated use of (52) and (56), we obtain

$$\begin{aligned}\boldsymbol{\beta}^{(k)}(z) &= \mathbf{P}^{(k)}(z, z_{k-1})\boldsymbol{\beta}(z_{k-1}) \\ &= \mathbf{P}^{(k)}(z, z_{k-1})\mathbf{P}^{(k-1)}(z_{k-1}, z_{k-2})\boldsymbol{\beta}(z_{k-2}) = \cdots \\ &= \mathbf{P}^{(k)}(z, z_{k-1})\left\{\prod_{j=k-1}^{j=1} \mathbf{P}^{(j)}(h_j, 0)\right\}\boldsymbol{\beta}(0),\end{aligned} \tag{57}$$

where $h_j = z_j - z_{j-1}$ is the thickness of the jth layer and the bracketed superscript denotes the layer number (note that when evaluated at the interfaces, $\boldsymbol{\beta}(z)$ does not need a bracketed superscript since it is continuous across the interfaces). Equation (57) shows that when $\boldsymbol{\beta}(z)$ is known at the bottom surface, its value at any other point in any layer is completely determined. Let $z = h$, $k = N$. We obtain

$$\boldsymbol{\beta}(h) = \left\{\prod_{j=N}^{j=1} \mathbf{P}^{(j)}(h_j, 0)\right\}\boldsymbol{\beta}(0), \tag{58}$$

which relates the values of $\boldsymbol{\beta}$ at the top and bottom surfaces. The vectors $\boldsymbol{\beta}(0)$ and $\boldsymbol{\beta}(h)$ have 12 components in total. For a given problem, six of these components will be given as displacement or stress boundary conditions; the other six components can then be determined from (58). As an illustrative example, we assume that on the bottom and top surfaces, either the displacement or the surface tradition is given. If we define $\boldsymbol{\beta}_1(z)$ and $\boldsymbol{\beta}_2(z)$ by

$$\boldsymbol{\beta}_1(z) = \begin{Bmatrix} U \\ V \\ W \end{Bmatrix}, \quad \boldsymbol{\beta}_2(z) = \begin{Bmatrix} \hat{\tau}_{xz} \\ \hat{\tau}_{yz} \\ \hat{\sigma}_z \end{Bmatrix},$$

eqn (58) then yields

$$\left.\begin{aligned}\boldsymbol{\beta}_1(h) &= \mathbf{D}_1\boldsymbol{\beta}_1(0) + \mathbf{D}_2\boldsymbol{\beta}_2(0) \\ \boldsymbol{\beta}_2(h) &= \mathbf{D}_3\boldsymbol{\beta}_1(0) + \mathbf{D}_4\boldsymbol{\beta}_2(0)\end{aligned}\right\}, \tag{59}$$

where $\mathbf{D}_1$ is the 3×3 matrix formed from the first three rows and columns of the 6×6 coefficient matrix in (58) and $\mathbf{D}_2, \mathbf{D}_3, \mathbf{D}_4$ are similarly formed. If, say, $\boldsymbol{\beta}_2(0)$ and $\boldsymbol{\beta}_2(h)$ are given as boundary conditions (corresponding to the surface tractions known on the top and bottom surfaces), the other two vectors $\boldsymbol{\beta}_1(0)$ and $\boldsymbol{\beta}_1(h)$ from (59b) are then given by

$$\boldsymbol{\beta}_1(0) = \mathbf{D}_3^{-1}[\boldsymbol{\beta}_2(h) - \mathbf{D}_4\boldsymbol{\beta}_2(0)],$$

and (59a). Once $\boldsymbol{\beta}(0) = (\boldsymbol{\beta}_1(0), \boldsymbol{\beta}_2(0))^{\mathrm{T}}$ has been determined, the vector $\boldsymbol{\beta}(z)$ at any point can then easily be calculated according to (57) and the vector $\gamma(z)$ can be calculated from (53). In this manner the stress and displacement fields are determined throughout the plate without the assembly or inversion of a $6N\times 6N$ matrix.

5. COMPARISON BETWEEN ASYMPTOTIC AND EXACT SOLUTIONS

In order to assess the accuracy of the asymptotic approach, we present in this section some specific results. The composite used in the following calculations is a typical carbon fibre–epoxy resin composite whose values of the elastic constants μ_{T}, μ_{L}, λ, α and β have been determined experimentally by Markham (1970) as follows [in units of 10^9 N m^{-2}, see also Spencer (1974)]:

$$\mu_{\mathrm{l}} = 5.66, \quad \mu_{\mathrm{t}} = 2.46, \quad \lambda = 5.64, \quad \alpha = -1.27, \quad \beta = 241.71. \tag{60}$$

With the use of the relations (3), we obtain

$$E_{\mathrm{l}} = 239.35, \quad E_{\mathrm{t}} = 7.53, \quad \nu_{\mathrm{lt}} = 0.27, \quad \nu_{\mathrm{tt}} = 0.53. \tag{61}$$

Correspondingly, we have $\varepsilon = 0.023$. When these values are used, eqn (19) yields $\sigma_1 = 1.817p$, $\sigma_2 = 1.239p$ for $q/p = 1$. The exact roots given by Pagano's (1970) eqn (21) are $m_{1,2,3} = 6.481p$, $1.248p$, $1.817p$. Thus apart from the fact that $\sigma_1 = m_3$ holds exactly [see the paragraph below eqn (41)], σ_2 approximates m_2 with an error less than 7.5%.

We first consider a single-layer plate which is subject to the boundary conditions

$$\begin{aligned} \tau_{xz} = \tau_{yz} = 0, \quad \sigma_z = \Omega \sin px \sin qy, \quad &\text{at} \quad z = h, \\ \tau_{xz} = \tau_{yz} = \sigma_z = 0, \quad &\text{at} \quad z = 0, \end{aligned} \tag{62}$$

where p and q are the same as those defined by eqn (8) and Ω is a constant. If we scale the displacement and stress components by Ω times the product of the appropriate sine and cosine functions shown in (33)–(40) (e.g. u is scaled by $\Omega \cos px \sin qy$), then the scaled displacement and stress fields only depend on the values of s and r [defined by eqn (12) with $\tilde{h}$ replaced by h] in addition to z/h. In all of the figures shown, we have used the same letters to denote the scaled quantities. We choose $s = 4$, $r = 5$ for the single-layer plate. In Fig. 1, we have shown the variation of the scaled displacement field along the thickness. There (and also in all other figures) the solid lines correspond to exact solutions and dashed lines correspond to asymptotic results. We have multiplied the displacement along the fibre direction by 10 to bring it to the same order of magnitude as the other two components. The agreement is extremely good. We can see that the boundary layer structure is most evident near the boundary $z = h$ where the displacement gradient is large. This may be a source of error for those approximation methods which assume linear or cubic variations for the displacement field across the thickness. Although the latter assumptions can be good approximations for isotropic or other materials which does not exhibit strong anisotropy, they may fail for the type of transversely isotropic materials, considered in this paper, which contains large displacement gradient boundary layers. In Figs 2(a,b) we have shown the

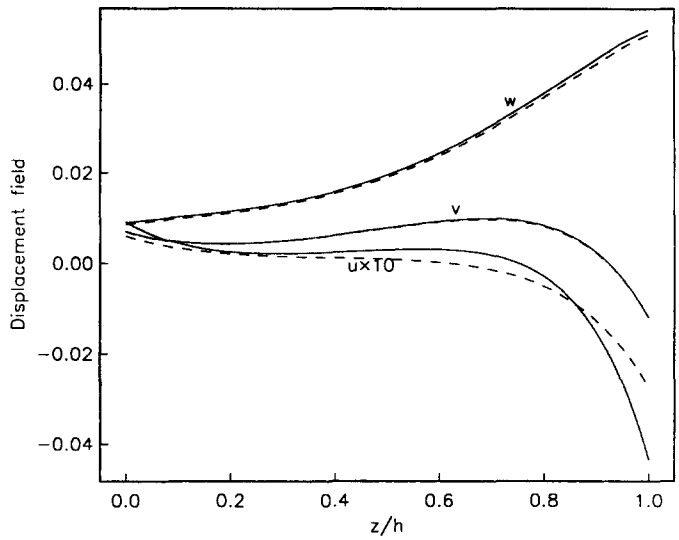

Fig. 1. Variation of the scaled displacement field across the thickness for a single-layer plate with $s = 4$, $r = 5$. Solid lines: exact solutions; dashed lines: asymptotic results.

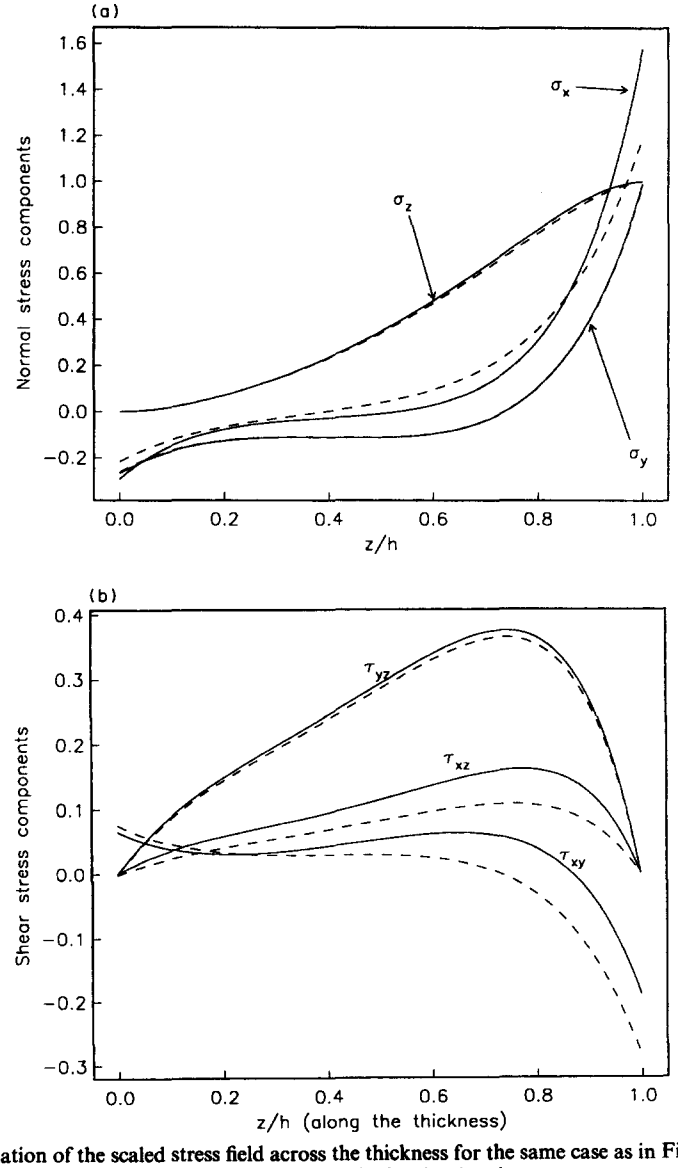

Fig. 2. Variation of the scaled stress field across the thickness for the same case as in Fig. 1; (a) for the normal stress components $\sigma_x, \sigma_y, \sigma_z$, (b) for the shearing stresses $\tau_{yz}, \tau_{xz}, \tau_{xy}$.

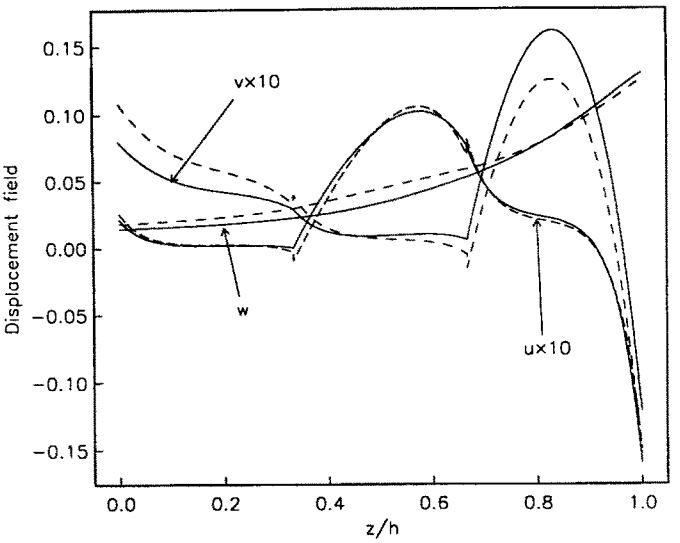

Fig. 3. Variation of the scaled displacement field across the thickness for a sandwich plate with $s = 3$, $r = 1$. Solid lines: exact solutions; dashed lines: asymptotic results. Interfaces are at $z = h/3$, $2h/3$.

variation of the scaled stress components across the thickness. The agreement is again very good, especially for the normal stress components. Figures 1 and 2 have a common feature: The asymptotic results for those displacement and stress components which involve the fibre direction are not as good as the results for those which do not involve the fibre-direction. For the former group (including u, σ_x, τ_{xz}, τ_{xy}), the asymptotic results seem to deviate from the exact solution most at the top surface. This may be because the contributions from higher order correction terms are most significant at $z = h$.

Next, we consider a sandwich plate under the same boundary conditions (62). The three layers are assumed to have equal thickness and the total thickness of the plate is given by h. The top and bottom layers have their fibers aligned with the x-axis, whilst the middle layer has its fibres along the y-direction. We use the definition (12) with $\tilde{h}$ replaced by $h/3$ and use the same scalings for the stress and displacement components as above. We choose $s = 3$, $r = 1$ in our calculations. In Figs 3–4, we have shown the variation of the scaled displacement and stress components along the thickness. We see that the asymptotic results have captured the overall behaviour of the two fields across the thickness and are especially good for σ_x.

6. DISCUSSIONS

In the above section, we have compared the asymptotic results with the exact solutions for a single-layer and a sandwich plate, using the experimentally measured values for the various elastic constants. The agreement is extremely good, bearing in mind the fact that the asymptotic method is only expected to be effective for very small values of ε while the value of ε which we have used is 0.023. In order to see how the agreement could be improved by assuming larger β values (or equivalently, larger E_l values), we have shown in Figs 5(a,b) the dependence on β of the scaled $(\sigma_x, \sigma_y, \tau_{xy})$ and (u, v, w) evaluated at the top surface $z = h$. We have only chosen these quantities because other quantities are either zero (τ_{xz} and τ_{yz}) or prescribed (σ_z) when the single-layer plate is subject to the boundary conditions (62). We see that the excellent agreement between the asymptotic and exact solutions for σ_y v and w are almost independent of the values of β (note that these quantities do not involve the fibre direction). For other quantities which involve the fibre direction, the asymptotic results for τ_{xy} and u converge to the exact solutions rapidly as β is gradually increased. The convergence for σ_x is not so good but we have to allow for the fact that the top surface is where the asymptotic result for σ_x deviates from the exact solution most, as can be seen from Fig. 2.

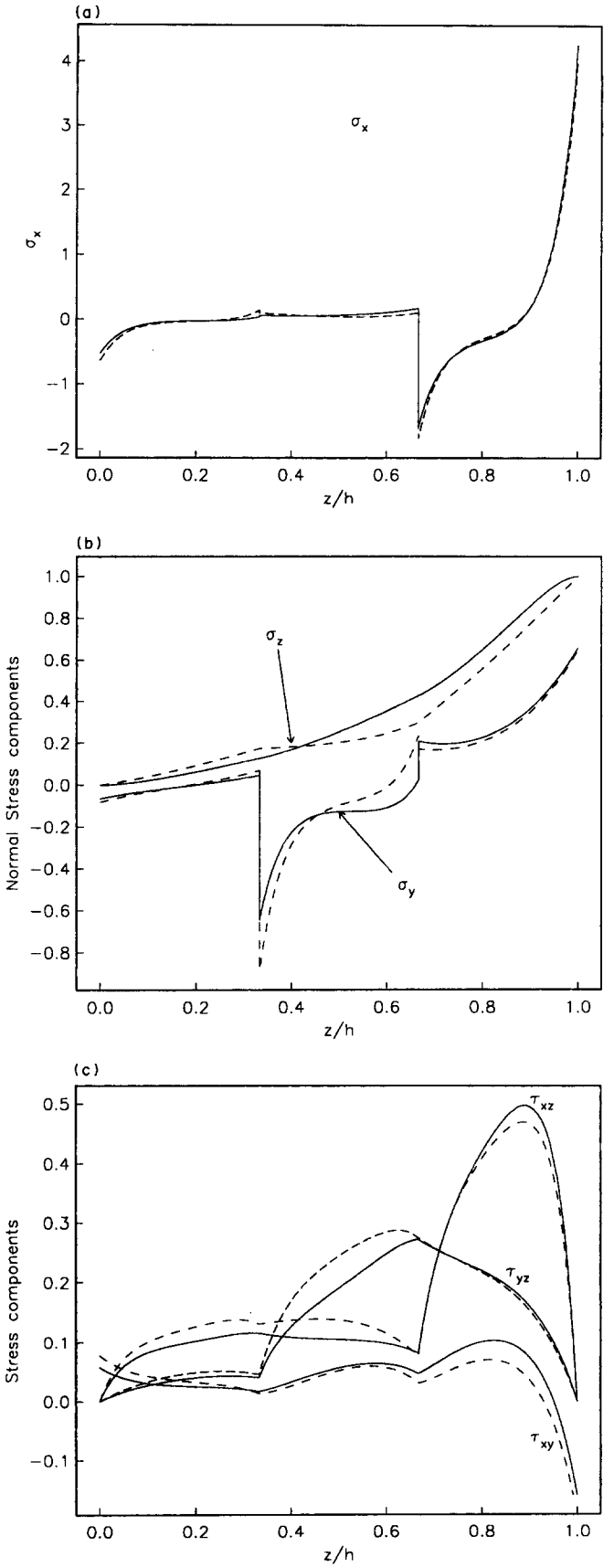

Fig. 4. Variation of the scaled stress field across the thickness for the same case as in Fig. 3; (a) for the normal stress component σ_x, (b) for the normal stress component; σ_y, σ_z, (c) for the shearing stresses $\tau_{yz}, \tau_{xz}, \tau_{xy}$.

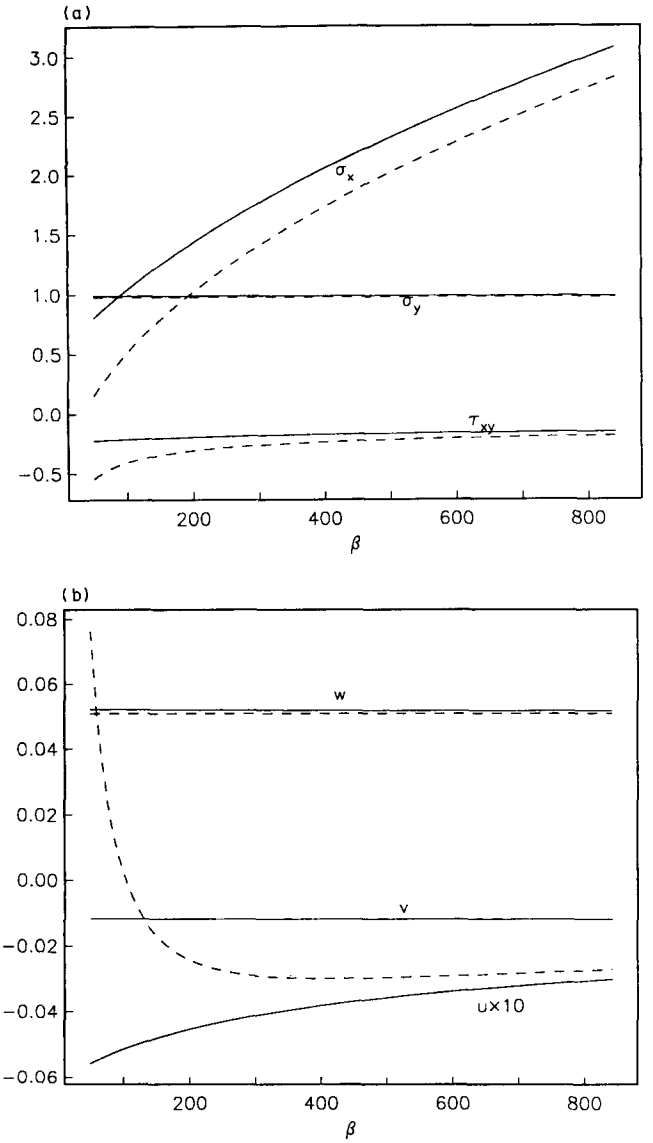

Fig. 5. Showing the convergence of the asymptotic solution for a single-layer plate towards the exact solution as β is gradually increased. Here $s = 4$, $r = 5$ and other elastic constants are fixed as given by (60) with fibres aligned with the x-axis; (a) for the scaled stresses $(\sigma_x, \sigma_y, \tau_{xy})$ evaluated at $z = h$, (b) for the scaled displacement $(u \times 10, v, w)$ evaluated at $z = h$.

We have also carried out calculations for two-layer and four-layer plates and by varying the values of s and r (recalling that our asymptotic analysis is based upon the assumption that both s and r are $O(1)$ quantities compared with ε). We find that in general, for the elastic constants given by (60), the asymptotic results give very good results for cases where s, the ratio of a/n to the thickness of each layer is not too large. This fact is also borne out by the following considerations.

We observe that in obtaining the leading order solution (14) from (9), we have implicitly assumed that both $\mu_L q^2 U$ and $\mu_L U''$ are small when compared with $p^2\beta$ (i.e. we have assumed s and r to be of order one relative to $1/\varepsilon$). Here U'' is of order U/h^2 with h denoting the thickness of the particular layer under consideration. Thus we expect that our leading order asymptotic analysis will deviate from the exact solution when either q^2/p^2 or $1/(p^2h^2)$ becomes comparable with β/μ_L. This is why the asymptotic analysis does not give good results for "thin" plates or plates composed of many thin layers. For example, for the two cases considered in the above section, the agreement with the exact solution becomes even better for smaller s values and less good for larger s values.

7. CONCLUSIONS

The stress analysis of laminated plates with simple support edge conditions is carried out in this paper by using an asymptotic method. By comparing the asymptotic results with the exact solutions, we showed that although the present asymptotic analysis may not be suitable for analysing laminated plates with many thin layers, it is nonetheless a very powerful tool for a single-layer thick plate or a thick laminated plate composed of only a few layers and can give very accurate results even if β/μ_L is only moderately large. Since this type of thick plate problems is where the classical plate theories fail most [and as the number of layers increases the classical plate theory gives better and better results (see Pagano and Hatfield, 1972)], the present asymptotic analysis does have some applicability and, where applicable, it provides a simple alternative to Pagano's exact analysis.

Finally, we remark that the asymptotic approach used in this paper not only gives simple asymptotic solutions, it also shows clearly the importance of those boundary layers across which certain displacement and stress components vary rapidly and where difficulty may arise in the application of finite element or finite difference methods.

Acknowledgements—The work of Y.B.F. is supported by a Nuffield Foundation Award for newly appointed science lecturers.

REFERENCES

Gilbert, F. and Backus, G. E. (1966). Propagator matrices in elastic wave and vibration problems. *Geophys.* **31,** 321–332.

Markham, M. F. (1970). Measurement of the elastic constants of fibre composites by ultrasonics. *Composites* **1,** 145–149.

Nayfeh, A. H. (1973). *Perturbation Methods.* Wiley, New York.

Owen, D. R. J. and Li, Z. H. (1987). A refined analysis of laminated plates by finite-element displacement methods—I. Fundamentals and static analysis. *Comput. Struct.* **26,** 907–914.

Pagano, N. J. (1970). Exact solutions for rectangular bidirectional composites and sandwich plates. *J. Compos. Mater.* **4,** 20–34.

Pagano, N. J. and Hatfield, S. J. (1972). Elastic behaviour of multilayered bidirectional composites. *AIAA Jl* **10,** 931–933.

Pipkin, A. C. (1979). Stress analysis for fibre-reinforced materials. *Adv. Appl. Mech.* **19,** 1–51.

Reddy, J. N. (1984). A simple higher-order theory for laminated composite plates. *J. Appl. Mech.* **51,** 745–752.

Spencer, A. J. M. (1974). Boundary layers in highly anisotropic plane elasticity. *Int. J. Solids Structures* **10,** 1103–1123.

Spencer, A. J. M. (1984). Constitutive theory for strongly anisotropic solids. In *Continuum Theory of the Mechanics of Fibre-reinforced Composites* (Edited by A. J. M. Spencer), pp. 1–32. Wien, New York.